Indolent mucinous tubular and spindle cell carcinoma of the kidney: A case report and review of the literature

GUANGRONG WU, JIAREN ZHANG, LIN JIANG, JIAJI LIU, LUNYOU ZHANG and WEI YANG

Department of Radiology, The First People's Hospital of Zunyi, The Third Affiliated Hospital of Zunyi Medical University, Zunyi, Guizhou 563000, P.R. China

Received February 7, 2023; Accepted July 10, 2023

DOI: 10.3892/ol.2023.13992

Abstract. Mucinous tubular and spindle cell carcinoma of the kidney (MTSCC) is a rare subtype of renal cancer. It consists of tubules separated by mucus stroma and a spindle cell. Few cases have been reported; thus, the imaging features of MTSCC are not well characterized. An MTSCC in the left kidney of a 65-year-old woman was incidentally discovered during a medical checkup. A review of the patient's medical history revealed that this kidney lump had an indolent growth process. The current study presented this case and reviewed the pathological features, imaging findings and treatment options of MTSCC to strengthen the recognition of this rare renal neoplasm by radiologists.

Introduction

Renal cell carcinoma (RCC), a large group of cancers originating from renal epithelial cells, includes ~10 subtypes based on molecular and histopathological characteristics (1). Mucinous tubular and spindle cell carcinoma (MTSCC) is a low-grade carcinoma composed of tightly packed tubules separated by pale mucinous stroma and a spindle cell component. MTSCC has low-grade malignant potential. Among RCCs, MTSCC is rare, accounting for <1% of all renal tumors (2). Additionally, MTSCC is slow-growing (3). The age distribution of patients with MTSCC is wide and these patients are predominantly female (2-5). Most patients have asymptomatic, incidentally discovered tumors (2). Some patients with uncommon histologic features, including mucin-poor stroma and high nuclear grade, may have painless gross hematuria or lower back pain (6). The overall imaging characteristics of MTSCC have not yet been clearly described.

Correspondence to: Professor Wei Yang, Department of Radiology, The First People's Hospital of Zunyi, The Third Affiliated Hospital of Zunyi Medical University, 98 Fenghuangbei Street, Zunyi, Guizhou 563000, P.R. China
E-mail: coxsackie@163.com

Key words: indolent mucinous tubular and spindle cell carcinoma of the kidney, computed tomography, magnetic resonance imaging, case report

Case report

Materials and methods

Image acquisition. Computed tomography (CT) examinations were performed with 64-slice spiral dual-energy CT (SOMATOM Definition Flash; Siemens Healthcare GmbH). The CT protocols were as follows: Non-contrast CT, corticomedullary phase (35 sec), nephrographic phase (60 sec) and dual-energy phase (300 sec). All CT examinations was performed using similar scanning parameters with tube voltage, 100 kV (non-contrast CT: 120KV); tube current, 300 mA; slice thickness, 5.0 mm; display field of view: 36.8x43.7 cm; reconstruction thickness, 1.5 mm. The contrast agent iohexol was intravenously injected at a dose of 1.5-2.0 mmol/kg via a power injector at an injection rate of 3.0 ml/sec.

Magnetic resonance imaging (MRI) examinations were performed with a 3.0-Tesla units (MAGNETOM Skyra; Siemens Healthcare GmbH). The MRI protocols were as follows: T1-weighted imaging (T1WI), T2-weighted imaging (T2WI), diffusion weighted imaging (DWI; slice thickness, 5 mm; gap, 1 mm; Display field of view, 38.0x44.9 cm), DWI (b value of 0 and 800 sec/mm^2, respectively), apparent diffusion coefficient (ADC) maps were reconstructed by subtracting the DWI with the high b value (800 sec/mm^2) from the DWI with the low b value (0 sec/mm^2). The present study was approved by the Ethics Committee of the First People's Hospital of Zunyi (Zunyi, China; approval no. 2023201). The patient provided written informed consent.

Histological and immunohistochemical methods. A piece of tissue (0.4 cm) was removed from the tumor. The biopsy material was fixed in 10% formalin (1 h; 25˚C). The tissue is gradually dehydrated in 75, 85 and 95% alcohol, and then it was made transparent in dimethylbenzene. The tissue were embedded in paraffin wax and cut into 3-μm sections. The tissue was stained with hematoxylin and eosin (10 min; 25˚C). Finally, the mount was sealed with neutral gum. The process of immunohistochemistry from sampling to embedding was the same as for histology, with the difference that the tissue was sectioned at 2 μm. Then, the sections were placed in a 65˚C oven for 30 min and dewaxed with dimethylbenzene (5 min; 2 times), dehydration with anhydrous ethanol (1 min; 2 times),

95% ethanol (1 min) and 85% ethanol (1 min) before being placed into a pressure cooker filled with sodium citrate buffer repair solution for 3 min. After rinsing, the sections were washed with phosphate buffer saline (PBS; 3 min; 3 times) and inactivated with 3% hydrogen peroxide (10 min; 25˚C), washed again in PBS (3 min; 3 times) and primary and secondary antibodies added for incubation (50 min; 37˚C), each incubation being followed by a rinse in PBS (3 min; 3 times). The color was developed with 3,3'-diaminobenzidine (5 min) and the reaction blocked. The sections were stained with hematoxylin (1 min; 25˚C) and differentiation with 1% hydrochloric alcohol (10 sec; 25˚C), rinsed with tap water (5 min; 25˚C) and dehydrated with 85 and 95% ethanol (2 min each; 25˚C) and, finally, with anhydrous ethanol (2 min; 2 times; 25˚C), cleared with dimethylbenzene (1 min; 25˚C) and sealed with neutral gum.

The catalog numbers of all primary and secondary antibodies were: RCC cat. no. GT210902, PAX8 cat. no. GT210202, vimentin (Vim) cat. no. GM072502, epithelial membrane antigen (EMA) cat. no. GM061302, CD10 cat. no. GT200402, CK8/18 cat. no. GT207802, HMB45 cat. no. GM063402, S100 cat. no. GT242002, Ki67 cat. no. GM724002, CD68 cat. no. GM081402 with secondary antibodies cat. no. Gk600711A (conjugated with horseradish peroxidase). Supplier of all primary and secondary antibodies was GeneTech (Shanghai) Co., Ltd. They were all ready-to-use antibodies and no dilution was required.

Literature review. In order to present the literature review, case reports of MTSCC in the English language were searched from the PubMed (pubmed.ncbi.nlm.nih.gov), Medline (lib.cpu.edu.cn/3b/12/c1172a80658/page.htm) databases. Key words were used for the search, which included 'mucinous tubular and spindle cell carcinoma of the kidney', 'mucinous tubular and spindle cell carcinoma', 'bilateral atrialmyxomas', 'mucinous tubular and spindle cell carcinoma of the renal', 'clinical', 'treatment' and 'image'. Inclusion criteria for screening studies were: Full text articles assessed for eligibility. Exclusion criteria for screening studies: duplicates removed, irrelevant publication, review only or full text not found.

Case. A 65-year-old woman with no painless gross hematuria or lower back pain was admitted to The First People's Hospital of Zunyi (Guizhou, China) on April 6, 2021 due to space-occupying lesions of the kidney found on conventional ultrasound images. The physical examinations performed on the patient at the time of admission included sight, touch, tapping and listening to check abdominal double renal areas. The double ureteral running areas were checked by touch and the bladder area with tapping and touch.

The laboratory tests were completed as follows: Serum myocardial zymogram, plasma D-dimer, troponin, blood routine, liver function, hepatitis B, hepatitis C, AIDS and syphilis antibody tests. Physical and laboratory examinations revealed no abnormalities. Then, the patient underwent abdominal enhanced CT and MRI. Enhanced CT has four stages: Noncontrast (NC), corticomedullary (CM), nephrographic (Ne) and excretory (Ex). The CT image showed an isodense mass with clear boundaries in the submiddle pole of the left kidney. A homogeneous solid soft mass 2.8x2.6x2.5 cm in size was identified on unenhanced CT (Fig. 1A). The Hounsfield units (HU) in the region of the mass were measured. In the NC, CM, Ne and Ex phases of the CT scan, the average attenuation values of the tumor were 21, 42, 61 and 69 HU, respectively. Dual-energy CT revealed iodine uptake within the lesion (Fig. 1D). Enhanced CT showed that the mass had mild to moderate, uniform, progressive enhancement (Fig. 1B and C). MRI revealed a round isointense lesion in the left kidney on T1-weighted imaging (T1WI; Fig. 2A). The mass was slightly hyperintense with a small hypointense area on T2-weighted imaging (T2WI; Fig. 2B). DWI (b=800 sec/mm^2) presented a high signal (Fig. 2C). The ADC (ADC=1.47x10^{-3} mm^2/sec) presented a low signal (Fig. 2D). DWI and the ADC indicated obviously restricted diffusion at the margin of the tumor. No obvious lipid content was observed in any of the MRI images. These imaging features suggested a diagnosis of renal cancer.

The patient then underwent laparoscopic left renal tumor removal. The mass was grayish-white and pale yellow with intact capsules. No invasion of the renal pelvis, perinephric fat or hilar vessels was observed. Neither the adrenal glands nor the lymph nodes showed signs of metastasis. In the histopathological examination of the lesion, mucinous tubular and spindle cells were found (Fig. 3A), and immunohistochemistry showed Vim (positive; Fig. 3B), PAX8 (positive; Fig. 3C), RCC (positive; data not shown), EMA (focally positive; Fig. 3E), Ki-67 (positive; ~5%), S-100 (negative), CD68 (negative), HMB45 (negative) (data not shown), CD10 (negative; Fig. 3F) and CK8/18 (negative; Fig. 3D). The patient was given anti-infection treatment by intravenous drip of cefoxitin, hemostasis treatment by intravenous drip of carbazochrome sodium sulfonate for injection, analgesia treatment by intravenous drip of propacetamo 1 hydrochloride for injection and nutritional support following the operation. The patient was discharged 4 days after the operation. At two and a half years following the operation, the chest and abdomen of the patient was reexamined by CT and no signs of tumor recurrence and metastasis were found (Fig. 1F).

The medical history of the patient was reviewed. This renal mass may have existed at 5 years from first presentation. The patient underwent chest CT, which revealed that the local renal parenchyma has protruded 1-2 mm on the lateral side of the left kidney due to thoracic trauma in 2016 (Fig. 1E).

Discussion

Previous reports have indicated the indolent behavior of MTSCC, with growth of 0.33 cm/year (3). In general, MTSCC has a better prognosis than other RCCs, including slower growth and significantly lower rates of progression, metastases and mortality (7). In the patient described in the present study, the left kidney local morphology was herniated five years ago, and the postoperative tumor size was 3.0x2.6x1.7 cm. According to the change in this mass size, it was concluded that this MTSCC was a slow-growing carcinoma. However, some MTSCCs of the kidney are highly malignant with locally advanced metastasis. Nephron-sparing surgery has been recommended for MTSCCs by a number of authors (8) and a number of studies have confirmed good long-term results and excellent patient survival (2,9).

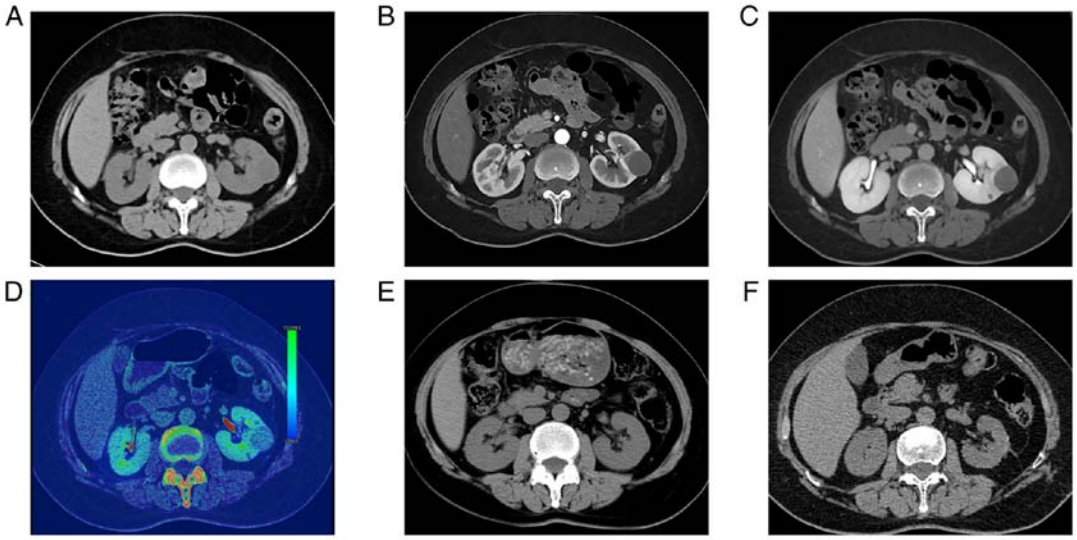

Figure 1. CT findings. (A) homogeneous solid soft mass 2.8x2.6x2.5 cm in size was identified with unenhanced CT; the average attenuation values of the tumor were 21, 42 and 61 HU on (A) noncontrast, (B) corticomedullary and (C) nephrographic images, respectively. The lesion showed mild to moderate, uniform, progressive enhancement. (D) Dual-energy CT revealed iodine uptake within the lesion. (E) Local morphology of the kidney had changed based on CT results from 2016 (arrow). (F) The image of the CT scan 2.5 years after the operation. CT, computed tomography; HU, Hounsfield units.

Histologically, MTSCCs are composed of a white mucinous matrix, long narrow tubular epithelial cells and spindle cells. Clear cell renal cell carcinoma is characterized by cells with clear cytoplasm and a delicate capillary network. Papillary renal cell carcinoma shows a focal papillary architecture. Renal collecting duct carcinoma presents irregular adenoid and small tubular structure, with high nuclear grade and evident nucleoli (10). In 2006, according to the percentage of extracellular mucin in the tumor after adequate sampling, Fine *et al* (8) expanded the histological spectrum of MTSCC into two variants: Classic, with ample mucin stroma, and mucin-poor, with little to no mucin. Classic tumors have an indolent behavior. Lack of mucin may be related to sarcomatoid transformation and metastasis. A few MTSCCs have been reported to exhibit sarcomatoid changes and high-grade epithelial elements (10). Some studies (10,11) have shown that the variability in the imaging features of MTSCCs is based on their histological diversity. The signal intensity on T2WI images is determined by the amount of mucin; the greater the amount of mucin is, the higher the signal intensity (11,12). In the current patient, the tumor had an obviously high signal on the T2WI image and contained a large amount of mucin.

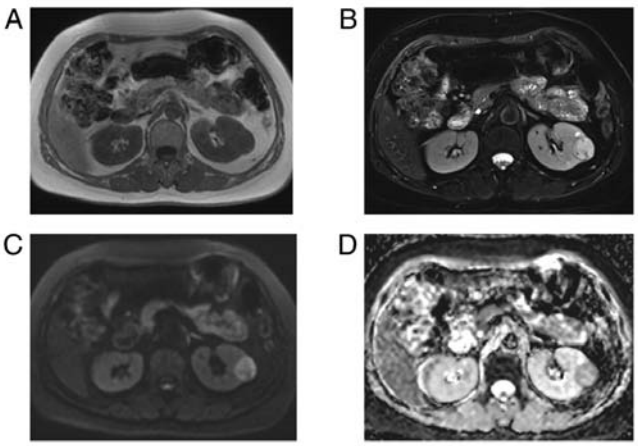

Figure 2. Magnetic resonance imaging findings. (A) An intense circumscribed round mass signal was detected in the left kidney on T1WI. (B) The mass was hyperintense with a small hypointense area on T2WI. (C) DWI (b=800 sec/mm^2) presented a high signal. (D) ADC presented a low signal (ADC=1.47 10^{-3} mm^2/sec). T1WI, T1-weighted imaging; T2WI, T2-weighted imaging; DWI, Diffusion weighted imaging; ADC, apparent diffusion coefficient.

Genetically, some studies have revealed that MTSCCs with aggressive clinical behavior have progressed through clonal evolution; CDKN2A/B deletion and additional complex genomic abnormalities may contribute to this process (13,14). Locally advanced/metastatic MTSCCs share typical MTSCC genomic profiles with loss of chromosomes 1, 4, 6, 8, 9, 13, 14, 15 and 22, while some exhibit additional complex genomic alterations, most frequently a relative gain of 1q (7/8) (14,15). Wang *et al* (16) identified VSTM2A and IRX5 as novel cancer-specific and lineage-specific biomarkers in MTSCC. Immunohistochemically, the neoplastic cells of both the tubules and spindle cells stain consistently positive for PAX2/8, low-molecular-weight cytokeratins (CK8/18, CK19 and CK7), EMA, alpha-methylacyl-CoA racemase and E-cadherin (17). In the present case report the results were Vim (positive), PAX8 (positive), RCC (positive), EMA (focally positive), Ki-67 (positive) and CK8/18 (negative). The present case was negative for CK8/18 but previous cases of MTSCC have been positive (17). The phenomenon may be the same as that of CD10 and CD15 described in Zhao *et al* (17), which are usually negative and occasionally positive. CD10 marker is sensitive to renal cell neoplasms derived from proximal tubules, including clear cell and papillary RCCs (18). Only 15% of the mucinous tubular and spindle cell carcinoma displayed immunoreactivity with CD10 (19). CD15 interacts with E-, L- and P-selectins, which allows for adhesion with endothelial cells. CK8/18 are the sole keratins present in the proximal tubular epithelial cells of the kidney (20). The negative expression of CD10, CD15 and CK8/18 in MTSCC is related to the histological structure and

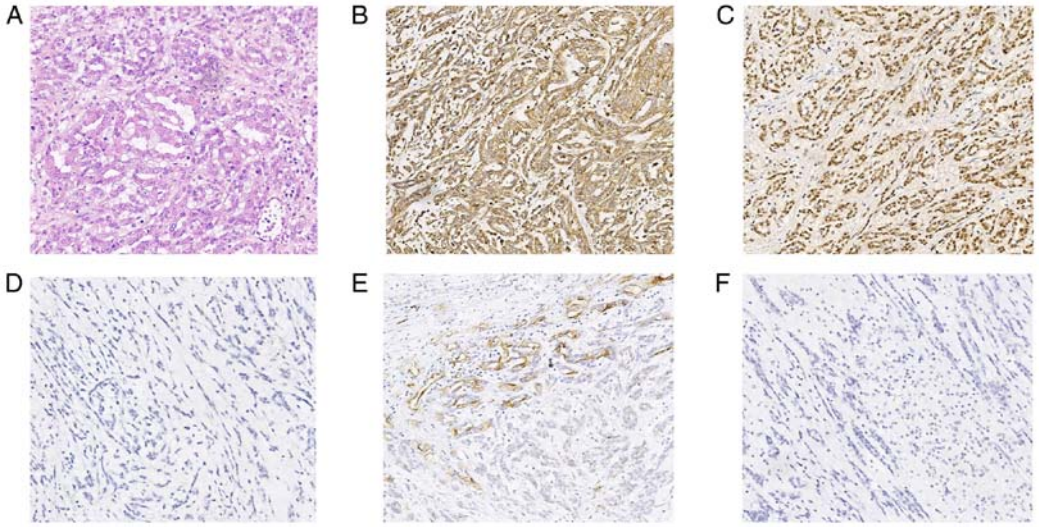

Figure 3. Histological and immunohistochemical findings. (A) The tumor is composed of white mucinous matrix, long narrow tubular epithelial cells and spindle cells (hematoxylin and eosin; magnification, x200). (B) Vimentin-positive (magnification, x100). (C) PAX8-positive (magnification, x100). (D) CD8/18 negative (magnification, x100). (E) Epithelial membrane antigen-positive (magnification, x100). (F) CD10-negative (magnification, x100).

differentiation degree of MTSCC (21). The positive expression of CD10, CD15 and CK8/18 in other tumors can represent that the tumor is malignant (20,22).

MTSCCs are usually a solitary, well-circumscribed, isodense mass originating from the renal medulla on CT imaging. They can be exophytic, partially exophytic, or endophytic tumors. Enhancement is less than that of the cortex and medulla in all CT phases and lesions show mild to moderate, uniform and progressive enhancement but may be homogenous when tumors are <5 cm (23). Dual-energy imaging can be used to distinguish mild enhancement from nonenhancement. Cystic components and calcification are rarely detected (24). Renal vein invasion, perinephric extension, and metastatic disease are extremely rare (4,5). However, in a few studies, metastasis has been reported in 10-27% of patients (9,25). Common metastatic sites include the lymph nodes, bone and retroperitoneum (13). The studies by Lu *et al* (24) and Zhu *et al* (26) show that MTSCCs are isodense or hypodense masses on unenhanced CT scans. In the present report, the mass was slightly hypodense. It was isointense on T1WI and usually had a high signal on T2WI (classical). DWI indicated a high signal; the ADC presented a low signal. Benign tumors of the kidney typically show low enhancement on contrast-enhanced CT imaging, high signal on DWI and low signal on ADC (27).

MTSCC, together with collecting duct carcinoma (CDC) and papillary renal cell carcinoma (PRCC), are thought to be hypovascular tumors due to their enhancement pattern. However, their treatment modalities and prognoses are different. Therefore, it is necessary for radiologists to differentially diagnose MTSCC, papillary RCC and CDC. PRCC is a slight hyperattenuating tumor; however, MTSCC is an isodense or hypodense mass. Some researchers consider that the pathological basis of hyperdensity on unenhanced CT is mainly hemosiderin deposition (24). PRCCs usually have calcification, necrosis and cystic changes on CT. Enhancement is greater with PRCC than with MTSCC tumors during all phases of CT. MTSCC is homogeneously slightly hyperintense, whereas PRCC is heterogeneously hypointense on T2WI. The T2 signal intensity ratio of MTSCC is 0.96, and that of PRCC is 0.67 (28). Most patients with MTSCC show homogeneous enhancement and no retroperitoneal lymph node metastasis, whereas those with CDC show heterogeneous enhancement and retroperitoneal lymph node metastasis. Normal renal cortex and medulla enhancement are more than MTSCC and CDC tumor enhancement in all phases of CT (5). However, the degree of enhancement of MTSCC is less than that of CDC in all phases.

As this type of tumor is rare, the best treatment scheme has yet to be properly determined. Nephrectomy and tumor cryoablation are performed in patients without metastasis and the effect of treatment is good. According to Li *et al* (3), follow-up observation and delayed treatment of patients with MTSCC does not reduce the 3-year survival rate or increase the recurrence rate. No therapeutic strategy has yet been established for metastatic MTSCC. One case report described the surgical removal of MTSCC with lymph node metastasis. One year after the operation, repeated imaging showed no signs of recurrence (7). It has been reported that sunitinib and the combination of nivolumab plus ipilimumab are effective in the treatment of metastatic patients (9,29). Ivey *et al* (7) demonstrated a large left renal mass and associated retroperitoneal lymphadenopathy on CT. The pathological features of the mass is a tubulocystic pattern with mucin interspersed with a spindle cell pattern. Ged *et al* (9) presented specific pathological features that high-grade histological features or sarcomatoid dedifferentiation were diagnosed in 5 of 6 patients with metastatic disease compared with 0 of 19 non-metastatic patients. There was revealed a large tumor at the upper pole of the left kidney with bone metastases on CT in Furubayashi *et al* (29). From these cases, it is known that MTSCC with high degree of malignancy is either a larger tumor or a higher histological grade. As far as the treatment results are concerned, compared with the treatment of patients in Ivey *et al* (7) and Li *et al* (3), there is no difference in the rate of recurrence one year after operation. Since the present patient's tumor was small, there were no high-grade histological features and metastases. The patient in the present case report lived longer and treatment

effect is superior compared with the treatment of patients in Ged *et al* (9) and Furubayashi *et al* (29).

Most patients are asymptomatic and tumors are found by accident. Some patients with uncommon histologic features may have painless gross hematuria or lower back pain. In the present case, the tumor was discovered by accident without any clinical symptoms. Previous case reports showed that MTSCC is an indolent tumor with a long course of disease (2,3). However, in previous case reports, it can be explained that there are no comprehensive image of the case with a long course of the tumor and a case report without an image cannot provide a longer course of the disease. The novelty of the present case lies in providing a morphological change of the patient's tumor for 5 years, dual-energy CT image, a comprehensive image consistent with the pathological diagnosis and postoperative reexamination image. The present case report can supplement the image performance of MTSCC. The limitation of the present study is that it does not include an image of the tumor after surgical removal.

MTSCCs grow slowly. Early in the cancer, the mass may not be visible, but the local morphology of the kidney may have changed based on CT images. However, MTSCCs are not always indolent tumors. It is necessary to raise radiologists' awareness of the risks of MTSCC. Any lump in the kidney or any localized change in the morphology of the kidney should be of concern to the radiologist. MTSCCs generally have low malignancy. Therefore, with improved preoperative diagnosis, nephron-sparing surgery should be considered as the principal treatment choice. This will be helpful in preserving the postoperative renal function of patients.

Acknowledgments

Not applicable.

Funding

No funding was received.

Availability of data and materials

All data generated or analyzed during this study are included in this published article.

Authors' contributions

GRW performed data collection and wrote the manuscript. JRZ and LJ were responsible for the analysis of case data and literature and edited the manuscript. JJL performed data collection. LYZ performed the staining of this tumor and provided the pathological procedures. WY performed data analysis and supervised the present study. WY and JJL confirm the authenticity of all the raw data. All authors agreed to the journal to which the article was submitted and agreed to take responsibility for all aspects of the work. All authors read and approved the final version of the manuscript.

Ethics approval and consent to participate

The present study was approved by the Ethics Committee of the First People's Hospital of Zunyi (Zunyi, China; approval no. 2023201). The patient provided written informed consent. The patient agreed to cooperate with us to have a chest/abdomen CT examination every year to observe the postoperative recurrence/metastasis. Thus, an ethical review was conducted.

Patient consent for publication

The patient provided written informed consent for the case study to be published.

Competing interests

The authors declare that they have no competing interests.

References

1. Moch H, Cubilla AL, Humphrey PA, Reuter VE and Ulbright TM: The 2016 WHO classification of tumours of the urinary system and male genital organs-part A: Renal, penile, and testicular tumours. Eur Urol 70: 93-105, 2016.
2. Xu X, Zhong J, Zhou X, Wei Z, Xia Q, Huang P, Shi C, Da J, Tang C, Cheng W and Ge J: Mucinous tubular and spindle cell carcinoma of the kidney: A study of clinical, imaging features and treatment outcomes. Front Oncol 12: 865263, 2022.
3. Li XS, Yao L, Gong K, Yu W, He Q, Zhou LQ and He ZS: Growth pattern of renal cell carcinoma (RCC) in patients with delayed surgical intervention. J Cancer Res Clin Oncol 138: 269-274, 2012.
4. Cornelis F, Ambrosetti D, Rocher L, Derchi LE, Renard B, Puech P, Claudon M, Rouvière O, Ferlicot S, Roy C, *et al*: CT and MR imaging features of mucinous tubular and spindle cell carcinoma of the kidneys. A multi-institutional review. Eur Radiol 27: 1087-1095, 2017.
5. Wu J, Zhu Q, Zhu W, Chen W and Wang S: Comparative study of CT appearances in mucinous tubular and spindle cell carcinoma and collecting duct carcinoma of the kidney. Br J Radiol 88: 20140434, 2015.
6. Nathany S and Monappa V: Mucinous tubular and spindle cell carcinoma: A review of histopathology and clinical and prognostic implications. Arch Pathol Lab Med 144: 115-118, 2020.
7. Ivey JA III, Cortese C, Baird BA, Thiel DD and Lyon TD: Mucinous tubular and spindle cell carcinoma of the kidney with nodal metastasis managed with surgical resection. Eur Urol Open Sci 29: 10-14, 2021.
8. Fine SW, Argani P, DeMarzo AM, Delahunt B, Sebo TJ, Reuter VE and Epstein JI: Expanding the histologic spectrum of mucinous tubular and spindle cell carcinoma of the kidney. Am J Surg Pathol 30: 1554-1560, 2006.
9. Ged Y, Chen YB, Knezevic A, Donoghue MTA, Carlo MI, Lee CH, Feldman DR, Patil S, Hakimi AA, Russo P, *et al*: Mucinous tubular and spindle-cell carcinoma of the kidney: Clinical features, genomic profiles, and treatment outcomes. Clin Genitourin Cancer 17: 268-274.e1, 2019.
10. Trpkov K, Hes O, Williamson SR, Adeniran AJ, Agaimy A, Alaghehbandan R, Amin MB, Argani P, Chen YB, Cheng L, *et al*: New developments in existing WHO entities and evolving molecular concepts: The genitourinary pathology society (GUPS) update on renal neoplasia. Mod Pathol 34: 1392-1424, 2021.
11. Farghaly H: Mucin poor mucinous tubular and spindle cell carcinoma of the kidney, with nonclassic morphologic variant of spindle cell predominance and psammomatous calcification. Ann Diagn Pathol 16: 59-62, 2012.
12. Thway K, du Parcq J, Larkin JMG, Fisher C and Livni N: Metastatic renal mucinous tubular and spindle cell carcinoma. Atypical behavior of a rare, morphologically bland tumor. Ann Diagn Pathol 16: 407-410, 2012.
13. Yang C, Cimera RS, Aryeequaye R, Jayakumaran G, Sarungbam J, Al-Ahmadie HA, Gopalan A, Sirintrapun SJ, Fine SW, Tickoo SK, *et al*: Adverse histology, homozygous loss of CDKN2A/B, and complex genomic alterations in locally advanced/metastatic renal mucinous tubular and spindle cell carcinoma. Mod Pathol 34: 445-456, 2021.

14. Brandal P, Lie AK, Bassarova A, Svindland A, Risberg B, Danielsen H and Heim S: Genomic aberrations in mucinous tubular and spindle cell renal cell carcinomas. Mod Pathol 19: 186-194, 2006.
15. Cossu-Rocca P, Eble JN, Delahunt B, Zhang S, Martignoni G, Brunelli M and Cheng L: Renal mucinous tubular and spindle carcinoma lacks the gains of chromosomes 7 and 17 and losses of chromosome Y that are prevalent in papillary renal cell carcinoma. Mod Pathol 19: 488-493, 2006.
16. Wang L, Zhang Y, Chen YB, Skala SL, Al-Ahmadie HA, Wang X, Cao X, Veeneman BA, Chen J, Cieślik M, *et al*: VSTM2A overexpression is a sensitive and specific biomarker for mucinous tubular and spindle cell carcinoma (MTSCC) of the kidney. Am J Surg Pathol 42: 1571-1584, 2018.
17. Zhao M, He XL and Teng XD: Mucinous tubular and spindle cell renal cell carcinoma: A review of clinicopathologic aspects. Diagn Pathol 10: 168, 2015.
18. Truong LD and Shen SS: Immunohistochemical diagnosis of renal neoplasms. Arch Pathol Lab Med 135: 92-109, 2011.
19. Paner GP, Srigley JR, Radhakrishnan A, Cohen C, Skinnider BF, Tickoo SK, Young AN and Amin MB: Immunohistochemical analysis of mucinous tubular and spindle cell carcinoma and papillary renal cell carcinoma of the kidney: Significant immunophenotypic overlap warrants diagnostic caution. Am J Surg Pathol 30: 13-19, 2006.
20. Moll R, Divo M and Langbein L: The human keratins: Biology and pathology. Histochem Cell Biol 129: 705-733, 2008.
21. Ferlicot S, Allory Y, Compérat E, Mege-Lechevalier F, Dimet S, Sibony M, Couturier J and Vieillefond A: Mucinous tubular and spindle cell carcinoma: A report of 15 cases and a review of the literature. Virchows Arch 447: 978-983, 2005.
22. Szlasa W, Wilk K, Knecht-Gurwin K, Gurwin A, Froń A, Sauer N, Krajewski W, Saczko J, Szydełko T, Kulbacka J and Małkiewicz B: Prognostic and therapeutic role of CD15 and CD15s in cancer. Cancers (Basel) 14: 2203, 2022.
23. Kenney PA, Vikram R, Prasad SR, Tamboli P, Matin SF, Wood CG and Karam JA: Mucinous tubular and spindle cell carcinoma (MTSCC) of the kidney: A detailed study of radiological, pathological and clinical outcomes. BJU Int 116: 85-92, 2015.
24. Lu D, Yuan W, Zhu Q, Ye J, Zhu W and Chen W: Comparative study of CT and MRI appearances in mucinous tubular and spindle cell carcinoma and papillary renal cell carcinoma. Br J Radiol 94: 20210548, 2021.
25. Adamane SA, Menon S, Prakash G, Bakshi G, Joshi A, Popat P and Desai SB: Mucinous tubular and spindle cell carcinoma of the kidney: A case series with a brief review of the literature. Indian J Cancer 57: 267-281, 2020.
26. Zhu Q, Zhu W, Wang Z and Wu J: Clinical and CT imaging features of mucinous tubular and spindle cell carcinoma. Chin Med J (Engl) 127: 1278-1283, 2014.
27. Israel GM and Bosniak MA: How i do it: Evaluating renal masses. Radiology 236: 441-450, 2005.
28. Oliva MR, Glickman JN, Zou KH, Teo SY, Mortelé KJ, Rocha MS and Silverman SG: Renal cell carcinoma: t1 and t2 signal intensity characteristics of papillary and clear cell types correlated with pathology. AJR Am J Roentgenol 192: 1524-1530, 2009.
29. Furubayashi N, Taguchi K, Negishi T, Miura A, Sato Y, Miyoshi M and Nakamura M: Cytoreductive nephrectomy after combination of nivolumab plus ipilimumab for mucinous tubular and spindle cell carcinoma of the kidney with bone metastases: A case report. In Vivo 36: 510-521, 2022.